AGU Advances

RESEARCH ARTICLE
10.1029/2020AV000343

Outsize Influence of Central American Orography on Global Climate

Jane W. Baldwin[1], Alyssa R. Atwood[2], Gabriel A. Vecchi[3,4], and David S. Battisti[5]

[1]Lamont-Doherty Earth Observatory, Columbia University, Palisades, NY, USA, [2]Department of Earth, Ocean, and Atmospheric Science, Florida State University, Tallahassee, FL, USA, [3]Department of Geosciences, Princeton University, Princeton, NJ, USA, [4]High Meadows Environmental Institute, Princeton University, Princeton, NJ, USA, [5]Department of Atmospheric Sciences, University of Washington, Seattle, WA, USA

Key Points:

- Central American orography blocks easterlies and warms sea surface temperatures in the northern tropical East Pacific, shaping precipitation and the El Niño-Southern Oscillation
- Low biases in these mountains' height in climate models are partially responsible for pervasive tropical climate simulation biases
- These and other model biases are improved by alternative interpolation of topography onto model grids to better retain mountain height

Supporting Information:

Supporting Information may be found in the online version of this article.

Correspondence to:

J. W. Baldwin,
jbaldwin@ldeo.columbia.edu

Citation:

Baldwin, J. W., Atwood, A. R., Vecchi, G. A., & Battisti, D. S. (2021). Outsize influence of Central American orography on global climate. *AGU Advances*, *2*, e2020AV000343. https://doi.org/10.1029/2020AV000343

Received 12 NOV 2020
Accepted 8 MAR 2021

Author Contributions:

Conceptualization: Alyssa R. Atwood, Gabriel A. Vecchi, David S. Battisti
Funding acquisition: Alyssa R. Atwood, Gabriel A. Vecchi, David S. Battisti
Investigation: Alyssa R. Atwood, Gabriel A. Vecchi, David S. Battisti
Methodology: Alyssa R. Atwood, Gabriel A. Vecchi, David S. Battisti
Resources: Alyssa R. Atwood, Gabriel A. Vecchi
Supervision: Gabriel A. Vecchi

Abstract Global Climate Models (GCMs) exhibit substantial biases in their simulation of tropical climate. One particularly problematic bias exists in GCMs' simulation of the tropical rainband known as the Intertropical Convergence Zone (ITCZ). Much of the precipitation on Earth falls within the ITCZ, which plays a key role in setting Earth's temperature by affecting global energy transports, and partially dictates dynamics of the largest interannual mode of climate variability: The El Niño-Southern Oscillation (ENSO). Most GCMs fail to simulate the mean state of the ITCZ correctly, often exhibiting a "double ITCZ bias," with rainbands both north and south rather than just north of the equator. These tropical mean state biases limit confidence in climate models' simulation of projected future and paleoclimate states, and reduce the utility of these models for understanding present climate dynamics. Adjusting GCM parameterizations of cloud processes and atmospheric convection can reduce tropical biases, as can artificially correcting sea surface temperatures through modifications to air-sea fluxes (i.e., "flux adjustment"). Here, we argue that a significant portion of these rainfall and circulation biases are rooted in orographic height being biased low due to assumptions made in fitting observed orography onto GCM grids. We demonstrate that making different, and physically defensible, assumptions that raise the orographic height significantly improves model simulation of climatological features such as the ITCZ and North American rainfall as well as the simulation of ENSO. These findings suggest a simple, physically based, and computationally inexpensive method that can improve climate models and projections of future climate.

Plain Language Summary The Sierra Madre mountain range stretches north to south in Central America. These narrow mountains are important for climate due to their location. They block tropical winds that flow east to west, making winds slower and sea surface temperatures warmer in the tropical East Pacific. This affects tropical rainbands and a pattern of year-to-year climate variability in the tropical Pacific Ocean, called the El Niño-Southern Oscillation, which has impacts across the entire globe. Climate models break the earth up into grid boxes to simulate atmosphere and ocean circulations. Since mountain peaks are smaller than these grid boxes, mountains in climate models, including the Sierra Madre, are shorter than in reality. The low bias in these mountains makes the simulation of climate in the tropical East Pacific different than that observed on earth. We show that these differences can be resolved by making mountains in climate models as high as in reality. Making mountains higher in climate models is also helpful in other places, including North America where the Rockies have a big impact on the atmosphere. Resolving these mountain-related biases can help improve climate models, and our confidence in their simulation of future changes such as global warming.

1. Introduction

It is standard practice in Global Climate Models (GCMs) for observed orography to be averaged onto the model grid. For example, in a 50 × 50 km atmosphere/land resolution GCM (e.g., the GFDL CM2.5 Forecast-Oriented Low Ocean Resolution GCM [FLOR]), the orographic height in a given gridcell is based on the value of the observed height spatially averaged over the relevant 50 × 50 km area (see Section 2). This averaging process acts to maintain the mean height of the surface, but smooths out orographic peaks, making mountains "seen" by the GCM atmosphere shorter and less sharp than in reality. This smoothing is further exacerbated in lower resolution GCMs, including those that have been deployed in recent

Visualization: Alyssa R. Atwood, Gabriel A. Vecchi
Writing – review & editing: Alyssa R. Atwood, Gabriel A. Vecchi, David S. Battisti

Intergovernmental Panel on Climate Change assessments (e.g., the Community Climate System Model version 4 [CCSM4], 0.9° × 1.25° atmosphere/land resolution).

A dominant way orography impacts large-scale climate is by blocking atmospheric flows (Molnar et al., 2010), deflecting winds horizontally or vertically depending on the height of the orographic feature and the atmospheric stratification (Hoskins & Karoly, 1981; Valdes & Hoskins, 1991; White et al., 2017). Vertical deflection also steers the large-scale winds through vortex stretching (Holton, 1973). Recent studies have highlighted that even thin but high orographic features can exert mechanical impacts highly influential for diverse climatic features. For example, the Himalayas form a high wall that blocks cold and dry extra-tropical air from reaching the tropics, and it has been argued that this effect is more important in driving the Indian monsoon than influences of the larger Tibetan Plateau (Boos & Kuang, 2010). Mechanical blocking of wind is also an important component of the northern Tibetan Plateau's influence on the East Asian Summer Monsoon (Chiang et al., 2015; Kong & Chiang, 2020), the Yunnan-Guizhou Plateau's influence on the Indian monsoon (Shi et al., 2016), and the Mongolian Plateau's influence on stationary wave patterns (White et al., 2017).

Outside of Asia, mechanical influences of Central American orography have been shown to influence sea surface temperatures (SSTs) in the northeastern Pacific (Kessler, 2006). The tropical easterlies in the Atlantic are generally blocked by the Sierra Madre, which is a major mountain range that runs northwest-to-southeast across Mexico and extends southward over Central America (Figures 1a and 1b). Three lower elevation

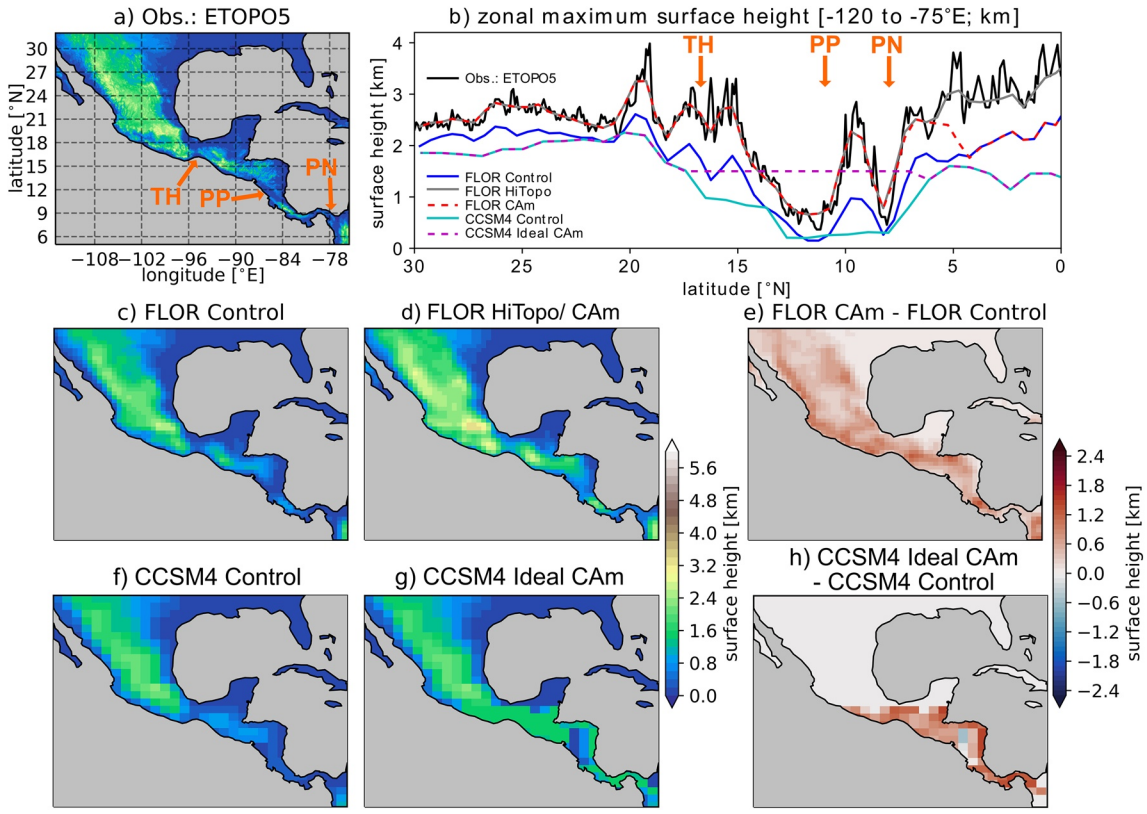

Figure 1. Surface height across Central America in observations compared to the boundary conditions in FLOR and CCSM4. Surface height over Central America is shown from the ETOPO5 5′ observed topography data set (a), and for the FLOR Control (c), FLOR CAm (d), CCSM4 Control (f), and CCSM4 Ideal CAm (g) simulations. Differences in surface height are shown for FLOR CAm and FLOR Control (e) and the CCSM4 Ideal CAm and CCSM4 Control simulations (h). The zonal maximum surface height across Central America (b) is also shown for the observations (black) and each model run—FLOR Control (blue), FLOR HiTopo (gray), FLOR CAm (dashed red), CCSM4 Control (cyan), and CCSM4 Ideal CAm (dashed magenta). Where different boundary conditions are the same appears as multi-colored due to layering of dashed and solid lines. Note that FLOR HiTopo and FLOR CAm boundary conditions are identical within Central America, but in other locations FLOR CAm follows the FLOR Control surface height while FLOR HiTopo is further elevated (see Section 2). In (a) and (b), the locations of the Central American low-elevation gaps are designated with orange arrows and lettering. CCSM4, Community Climate System Model version 4; FLOR, Forecast-Oriented Low Ocean Resolution; PN, Panama; PP, Papagayo; TH, Tehuantepec.

orographic gaps in the Sierra Madre (from north to south: the Tehuantepec, the Papagayo, and the Panama; Figures 1a and 1b) give rise to local wind jets in the tropical East Pacific and persistent wind stress (Chelton et al., 2004). This wind stress and its curl in turn drive cool SSTs outside of these gaps through increased air-sea heat fluxes and Ekman pumping (Steenburgh et al., 1998; Sun & Yu, 2006; S.-P. Xie et al., 2005). These mechanical effects of Central American mountains have also been shown to affect regional precipitation. For example, a combination of the cooling effect of these jets and subsidence driven by the Central American orography leads the local Intertropical Convergence Zone (ITCZ) to be displaced to the southern edge of the eastern Pacific warm pool in boreal winter (H. Xu et al., 2005). In addition to affecting eastern Pacific regional climatology, variation in these gap winds link low-frequency variability of the Atlantic/Arctic and low-frequency variability of the Pacific ocean (Karnauskas, 2014; Karnauskas et al., 2008; S.-P. Xie et al., 2007, 2008), and control interannual variations in eastern Pacific tropical cyclone frequency (Fu et al., 2017).

Despite their substantial impacts on climate, Central American mountains' height is poorly captured in most GCMs. GCMs have increased in resolution across model intercomparison projects (MIPs), resulting in improved resolution of mountain height. However, most GCMs today still exhibit substantial biases in the height of Central American mountains (Figure S1). Representing each MIP by its median GCM resolution, the resolved zonal maximum height of Central American mountains is ∼53% of their actual height in CMIP3 and CMIP5, and ∼75% in CMIP6 (Figure S1h). In the present day highest resolution GCMs (captured by HighResMIP; similar resolution to FLOR), the maximum height of Central American mountains is ∼88% of their actual height. Overall, resolved topography in the thin spit of Central America near the equator remains too low, likely limiting blocking of the prevailing easterlies.

The importance of mechanical impacts of mountains across the globe, and especially in Central America, suggests that the smoothing of orography in GCMs might be a significant source of model bias. To test this hypothesis, we make an alternative assumption in regridding observed orography to the GCM grid: in each 50 × 50 km FLOR gridcell we select the highest point from a 5 × 5 min resolution observed orographic data set, and choose that to be the height of the relevant gridcell (see Section 2). Compared to the standard averaging practice, this represents a rather extreme alternate assumption. It has the advantage of better capturing peak mountain height in the model, but creates broad regions at higher elevation than in reality (Figure 1b). The weather modeling community has explored alternative orographic interpolation schemes similar to this, that is, envelope orography (Jarraud et al., 1986; Wallace et al., 1983), but such methods are not common in atmosphere-ocean coupled climate modeling.

To test the effect of this alternate high orography on climate we run three simulations with GFDL CM2.5-FLOR: (1) a control simulation with standard present day orography ("FLOR Control"; Figure 1c, Figure S2b), (2) a simulation where this high orography modification is implemented everywhere on land ("FLOR HiTopo"; Figure S2c), and (3) another simulation where this modification is only done over Central America ("FLOR CAm"; Figure 1d). We also investigate additional simulations with the lower resolution 1° CCSM4: a control with standard orography ("CCSM4 Control"; Figure 1f), and a simulation with idealized elevated orography over Central America ("CCSM4 Ideal CAm"; Figure 1g) (Atwood et al., 2020). The CAm simulations are completed to test the hypothesis that the Central American orography has an outsize influence on climate and that low biases in orography over Central America are particularly influential in biasing the simulated tropical Pacific climatology.

2. Methods

The simulations, datasets, and analysis methods used in this study are described below.

2.1. GCM Simulations

Two GCMs are used in this study—CCSM4 and CM2.5-FLOR. Both are fully coupled atmosphere-ocean models. CCSM4 was developed at the National Center for Atmospheric Research, and has horizontal resolutions of 0.9 × 1.25° in the atmosphere/land and nominal 1 × 1° in the ocean (uniform 1.1° in longitude, variable in latitude from 0.27° at the equator to 0.54° at 33° latitude) (Deser et al., 2012; Gent et al., 2011). CESM has superseded CCSM4, but equivalent CCSM4 experiments can be run from the CESM1 code base

by using the CCSM4 component set, which includes the CAM4 atmosphere model (Hurrell et al., 2013). In this study, the 1300-year 1850 Control simulation of CCSM4 was employed (Gent et al., 2011), while the elevated orography experiment was performed with the CESM 1.0.5 code base using the CCSM4 component set (B_1850_CN). CM2.5-FLOR (hereafter "FLOR") was developed at NOAA's Geophysical Fluid Dynamics Laboratory, and features a rather high resolution approximately 50 × 50 km atmosphere/land using a cubed-sphere finite volume dynamical core (Putman & Lin, 2007), and a relatively lower resolution 1 × 1° ocean (telescoping to 0.333° meridional spacing near the equator). FLOR, which stands for "Forecast-oriented Low Ocean Resolution," has been shown to have improved skill in simulating precipitation climatology, extreme heat and rainfall events, and seasonal forecasting compared to lower resolution models similar to CCSM4 (Jia et al., 2014, 2016; Krishnamurthy et al., 2018; van der Wiel et al., 2016).

Orographic boundary conditions play a few different roles in GCMs, controlling surface height that the resolved atmospheric circulation interacts with, and parameterizations for sub-gridscale processes including gravity wave drag, boundary layer roughness, and aspects of the land model such as vegetation type and river flow. The focus of this study is on mechanical influences of orography on atmospheric circulation, so we alter just the boundary condition controlling surface height. Gravity wave drag and boundary layer roughness depend on parameterizations based on subgridscale variance of topography, which is kept identical in the Control and modified orography experiments. Static rather than dynamic vegetation is used, such that the vegetation type does not respond to the orographic alterations.

In the Control simulations of each GCM ("FLOR Control" and "CCSM4 Control"), radiative forcing is kept constant at pre-industrial levels (1860 in FLOR, 1850 in CCSM4), and standard orography is used. In these experiments, which reflect typical GCM treatment of orography, the orographic height in a given gridcell is the area-average of observed height in that gridcell.

We also run a few different perturbation experiments with non-standard orography but retaining pre-industrial radiative forcing. With FLOR, we instead set orography in each gridcell to be the maximum observed height across the relevant gridcell, an experiment we refer to as "FLOR HiTopo." The observed orography used is the ETOPO5 5 × 5′ resolution data set available from NOAA's National Center for Environmental Information. This type of alternative topographic interpolation was also performed over a limited area in a recent study that focuses on the effects of the Andes (W. Xu, 2019). To isolate the effect of Central American orography, we run an additional experiment in which orography is elevated only over Central America ("FLOR CAm"), specifically over two adjacent regions 14–32°N, 113-85°W, and 5–14°N, 95–75.5°W. Note that the resultant FLOR HiTopo and FLOR CAm surface height while much higher than that of FLOR Control is slightly lower than observed mountain peak height (Figure 1b), due to regridding from the regular lat-lon of the topography data to the GCM cubed-sphere grid.

The FLOR simulations begin with a "cold start," in which temperature and other values start out as constant throughout the atmosphere, and then dynamically spin up over the first few time steps. We previously found a "cold start" allowed the GCM to more robustly adjust to different orographic boundary conditions compared to providing atmospheric initial conditions from a preexisting simulation (J. W. Baldwin et al., 2019). We run each simulation for 200 years, analyzing years 31 to 200 to allow for model spin-up.

In the CCSM4 perturbation experiment, the height of the mountains across Central America were raised to 1,500 m (between 7 and 18°N, 120 and 76°W; Figure S2) (Atwood et al., 2020). Because the intent of this (earlier) orography modification was simply to reduce the tropical SST and low-level wind biases in the eastern Pacific associated with poor resolution of Central American orography, rather than improve the representation of Central American orography, we refer to this simulation as "CCSM4 Ideal CAm." This simulation was branched from year 863 of the 1300-year-long pre-industrial CCSM4 Control simulation, then run for 300 years. For CCSM4 Control years 1201–1300 are analyzed, whereas for CCSM4 Ideal CAm all 300 years simulated are analyzed.

2.2. Observed Datasets

A variety of observed climate datasets are used to compare to the model simulations and evaluate biases. Below we provide some summary information on these data sources, including the time periods we utilize for analysis. We use zonal and meridional wind and surface wind stress data from the Modern-Era

Retrospective analysis for Research and Applications, Version 2 (MERRA-2; 0.5° × 0.625°; 1/1980–12/2019; Gelaro et al. [2017]). We use SSTs from two data sources: the Hadley Centre Global Sea Ice and SST data set version 1.1 (HadISST; 1° × 1°; 1/1947–12/2019; Rayner et al. [2003]), and the Extended Reconstructed SST version 5 (ERSSTv5; 2° × 2°; 1/1947–12/2019; Huang et al. [2017]). Note that while data is available prior to 1947 for these SST datasets, we truncate the data at that year due to known uncertainties around the World War II period Chan & Huybers (2020). For ocean surface currents we use the Ocean Surface Current Analysis Real-time data at 15 m depth (OSCAR; 0.33° × 0.33°; Bonjean and Lagerloef [2002]). Finally, we use three different precipitation datasets: the Integrated Multi-satellitE Retrievals for GPM (IMERG; 10 km/0.1°; 1/2001–12/2018; Huffman et al. [n.d.]), the CPC Merged Analysis of Precipitation (CMAP; 2.5° × 2.5°; 1/1979–12/2018, P. Xie and Arkin [1997]), and the Global Precipitation Climatology Project monthly precipitation data set version 2.3 (GPCP; 2.5° × 2.5°; 1/1979–12/2017; Adler et al. [2003]).

2.3. ENSO Metrics

In assessing the fidelity of El Niño-Southern Oscillation (ENSO) simulation, our analysis of the monthly SST data proceeds as follows. We first linearly detrend the data, then remove the seasonal cycle to calculate anomalies, and finally average those anomalies over the the Niño 3 and Niño 3.4 regions (respectively, −5 to 5°N, 150 to 90°W, and −5 to 5°N, 170 to 120°W). These raw SST anomalies are used to determine the ENSO variance by month, whereas 3-month running means of the SST anomalies are used for calculating the ENSO power spectra.

2.4. Seasonal Average Analyses

We focus on the season of March–April–May (MAM) for our analysis and discussion, as this is the season that exhibits the largest East Pacific double ITCZ bias in both FLOR and CCSM4. During MAM, zonal mean precipitation in observations is stronger north of the equator and weaker south of the equator, whereas in both FLOR and CCSM4 Control simulations MAM precipitation is stronger to the south and weaker to the north (Figure 2). In contrast, September–October–November (SON) exhibits less bias, with a strong northern maximum in precipitation in both GCMs and observations. December–January–February (DJF) and June–July–August (JJA) seasonal averages for zonal mean precipitation (not shown) lie between that of MAM and SON.

In many of the following seasonal average figures we compare GCM biases to the effects of mountains in the GCM simulations. According to our hypothesis that increasing mountain height should reduce GCM biases, we expect the effect of higher mountains (i.e., CAm minus Control or HiTopo minus Control) to exhibit similarity to the inverse of the GCM biases (i.e., Obs. minus Control). To most clearly show this correspondence, in our figures we compare the effect of higher mountains to −1 × (GCM biases); if our hypothesis is true the maps should be similar. We label the figures accordingly, but note to guide the reader that as a result in some of the following maps warm/wet/strong-wind GCM biases show up as negative values and cool/dry/low-wind GCM biases show up as positive values.

3. Results

Consistent with previous work, we find large biases in the GCMs' simulation of eastern Pacific climate. In Central America, the southern extension of the Sierra Madre is known to block the flow of tropical easterly winds except in the few lower elevation gaps in the mountains. In many GCMs, including FLOR and CCSM4, low-level trade winds in the East Pacific proximal to these mountains are biased too strong (Song & Zhang, 2020) (Figures 3a and 3c), leading to negative SST biases in this region (Figures 3b and 3d). The negative SST bias is most pronounced where observed topography is high between the Tehuantepec and Papagayo gaps, and between the Papagayo and Panama gaps. North and south of this cold bias, there are also positive SST biases, which are adjacent to the Baja California Peninsula and along the western coast of South America, respectively. In the lower resolution CCSM4 Control the warm biases to the south and especially north of it (off the coast of Baja) are generally stronger and broader than in the FLOR Control.

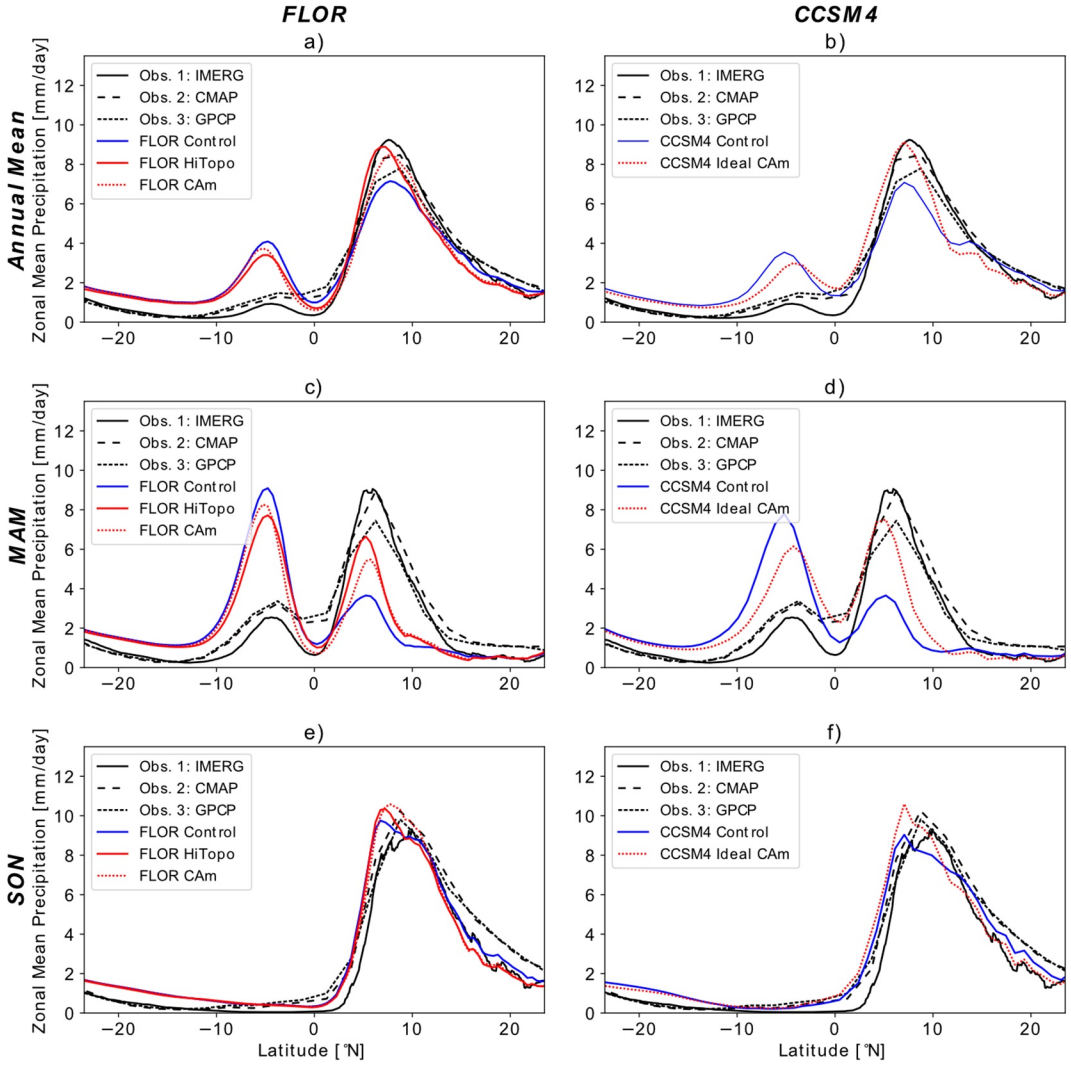

Figure 2. Eastern tropical Pacific zonal mean precipitation. Precipitation averaged over ocean grid points between 130 and 75°W is plotted for the annual mean (a and b), MAM seasonal mean (c and d), and SON seasonal mean (e and f). In all panels, black lines plot three different gridded observations (IMERG in solid black, CMAP in wide black dashes, and GPCP in small black dashes). In the left column, the colored lines plot FLOR Control (blue), FLOR HiTopo (red), and FLOR CAm (dashed red). In the right column, the colored lines plot CCSM4 Control (blue) and CCSM4 Ideal CAm (dashed red). CCSM4, Community Climate System Model version 4; FLOR, Forecast-Oriented Low Ocean Resolution; MAM, March–April–May; SON, September–October–November.

The raised orography in FLOR HiTopo leads to reduced biases in near-surface winds and SSTs, especially in the tropical East Pacific and to some degree in the western tropical Atlantic and Gulf of Mexico (Figures 3a, 3b, 3e, and 3f). These wind and SST bias reductions are also seen in FLOR CAm and CCSM4 Ideal CAm, indicating that the elevated Central American orography is responsible for these improvements (Figures 3g–3j). In all three simulations with altered orography, raised Central American mountains increase blocking of tropical easterlies, reducing wind speed over the northern tropical East Pacific. This decreased wind speed in turn leads to warmer SSTs through a combination of reduced latent and sensible heat fluxes from the ocean surface, and reduced upwelling and entrainment of deeper cold waters. To the west of Central and South America, these changes in the surface winds and SSTs substantially decrease the model biases compared to observations, with the strongest effects during MAM when the Pacific ITCZ is at its southern-most position and the trade winds north of the equator in the tropical East Pacific are correspondingly strong and northeasterly (Figure 3). In contrast, these mountains' effects on model biases are weakest

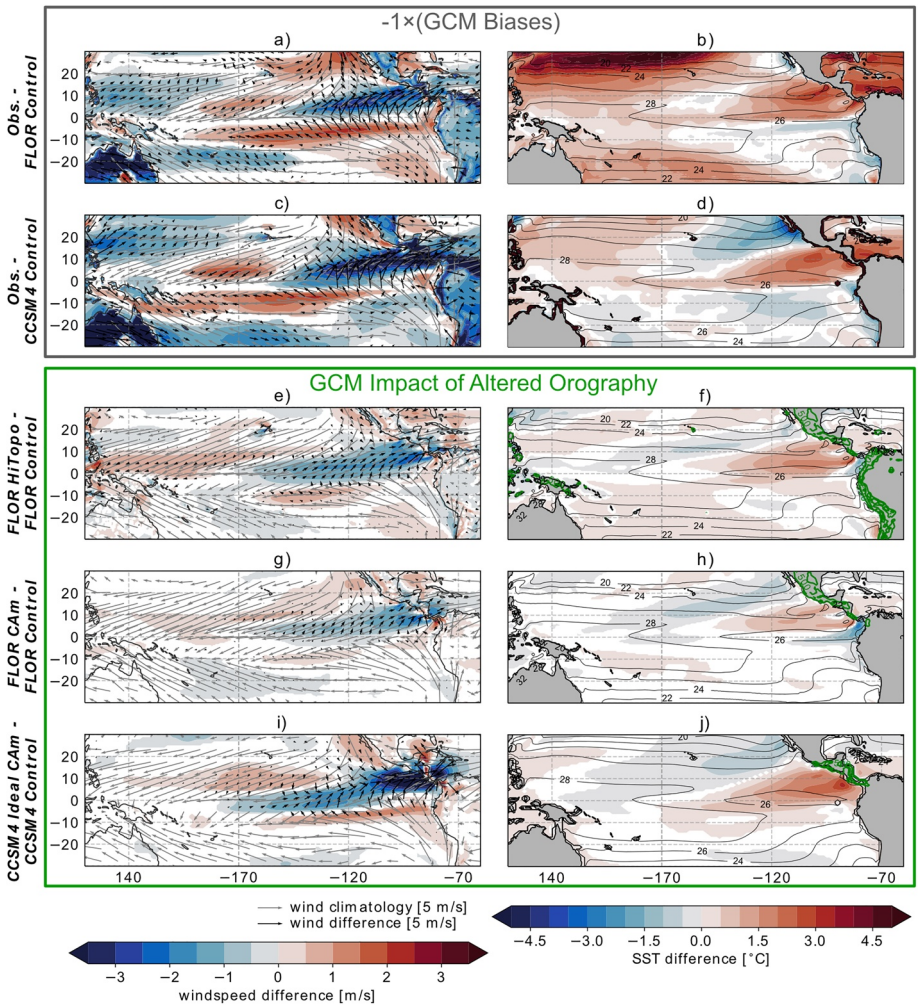

Figure 3. Influence of orography on tropical Pacific winds and sea surface temperatures (SSTs) for March–May (MAM). MAM average wind vectors and speeds are shown in the left column (a, c, e, g, and i), with windspeed differences shaded, wind differences in black vectors, and the relevant Control wind climatology in gray vectors. Wind data is taken from the lowest atmospheric level available in the 3-D data from the MERRA-2 reanalysis ("Obs."—1,000 hPa), FLOR output (996.1 hPa), or CCSM4 output (992.6 hPa). MAM average SSTs are shown in the right column (b, d, f, h, and j) with SST differences shaded, and relevant Control climatology in black contours. The observed SST data is HadISST. In the lower right-column panels (f, h, and j) the difference in the surface height boundary conditions between the relevant perturbation simulations and Control simulations is contoured in green. In all panels, differences that are not significant at a 90% level based on a two-sided *t*-test are masked out (i.e., are white for the filled contours, and do not appear for the vectors).

in SON (Figure S3), when the Pacific ITCZ is at its northern-most position, and effects in DJF and JJA (not shown) are intermediate to those in MAM and SON.

To the north and south of this region of warming in FLOR HiTopo and FLOR CAm, and to the north in CCSM4 Ideal CAm, the raised orography results in cooler surface waters, some of which further reduce the SST biases in these regions (Figures 3f, 3h, and 3j). The cooling to the north near the Baja Peninsula is coincident with enhanced wind speeds likely caused by convergence and upward motion to the south, over the region of warmer SSTs adjacent to Central America. In FLOR HiTopo and FLOR CAm, cooling to the south originates directly outside of the Panama gap, suggesting that it results from enhanced wind flow through the gap due to elevated Central American orography; the fact that CCSM4 Ideal CAm does not have a Panama Gap and exhibits no cold anomaly in this region further supports this interpretation (Figures 1h and 3j). In contrast, in the FLOR and CCSM4 Control simulations a warm bias exists in the region south of

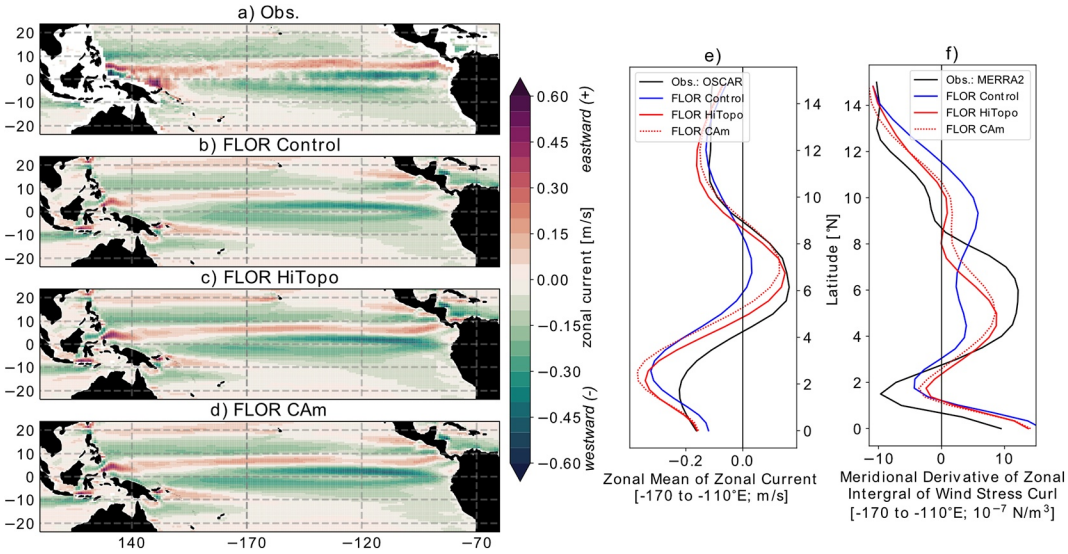

Figure 4. Zonal currents and related winds in FLOR. Time mean zonal currents across the tropical Pacific are shaded for observations (OSCAR; a), FLOR Control (b), FLOR HiTopo (c), and FLOR CAm (d). Before plotting, the OSCAR data (0.33 × 0.33°) is regridded to the FLOR ocean grid. To highlight and understand changes in the North Equatorial Counter Current (NECC), zonal means of these zonal currents are plotted for the northern tropics (e), and compared to the meridional derivatives of the zonal integrals of wind stress curl (f); in (e) and (f), observations are plotted in black, FLOR Control is blue, FLOR HiTopo is red, and FLOR CAm is dashed red.

the equator in the eastern Pacific (0–20°S, 150-85°W) that does not exhibit a clear connection to the Panama gap (Figures 3b and 3d).

In summary, the strong cool bias west of Central America and extending about 6,000 km into the tropical Pacific is clearly tied to orographic biases in Central America, as is some of the warm bias adjacent to the Baja California Peninsula. In contrast, the warm bias west of South America is not improved in these experiments, and may be associated with low-cloud biases not explored in this work.

In addition to impacting surface heat fluxes, altered orography over Central America also influences SSTs through its effects on oceanic circulation. The North Equatorial Counter Current (NECC) flows eastward at about 5–10°N in the Pacific (Figure 4a). It is weak and zonally truncated in the FLOR Control, but spans the Pacific with similar magnitude to observations in FLOR HiTopo and FLOR CAm (Figures 4b–4e). CCSM4 Ideal CAm also exhibits a more realistic magnitude NECC than CCSM4 Control, though the improvement is less dramatic than in the FLOR simulations (Figure S4). Sverdrup theory describes the NECC as arising from the meridional gradient in wind stress curl (Reid, 1948; Sverdrup, 1947), and these changes between simulations are consistent with changes in the wind stress curl. While in the FLOR Control the meridional gradient of wind stress curl proximal to the NECC is biased low, elevated orography alters this gradient to be closer to observations both in magnitude and position of the peak (Figure 4f). The NECC carries warm water from the west Pacific warm pool to the cooler tropical northeastern Pacific. In turn, in both FLOR HiTopo and FLOR CAm, the tropical northeastern Pacific SSTs are warmed by both the weakened local wind speeds and the strengthened NECC.

Biases in the simulation of tropical precipitation are partly driven by SST biases (Oueslati & Bellon, 2015; Samanta et al., 2019). Thus, the improvements in simulation of winds and SSTs west of Central America in the raised orography simulations should result in more realistic precipitation in the eastern Pacific. Indeed, compared to the Control simulations, in FLOR HiTopo, FLOR CAm, and CCSM4 Ideal CAm, precipitation increases greatly in the northeastern tropical Pacific and decreases slightly in the southern branch of the ITCZ (Figure 5), effectively shifting the eastern Pacific ITCZ northward (Figure 2). These effects are strongest during boreal spring (MAM; Figure 5), when the double ITCZ bias is also the most prominent, and weakest during boreal fall (SON; Figure S5), with summer and winter (JJA and DJF—not shown) exhibiting responses between the other two seasons. The northward ITCZ shift is associated with a southerly wind

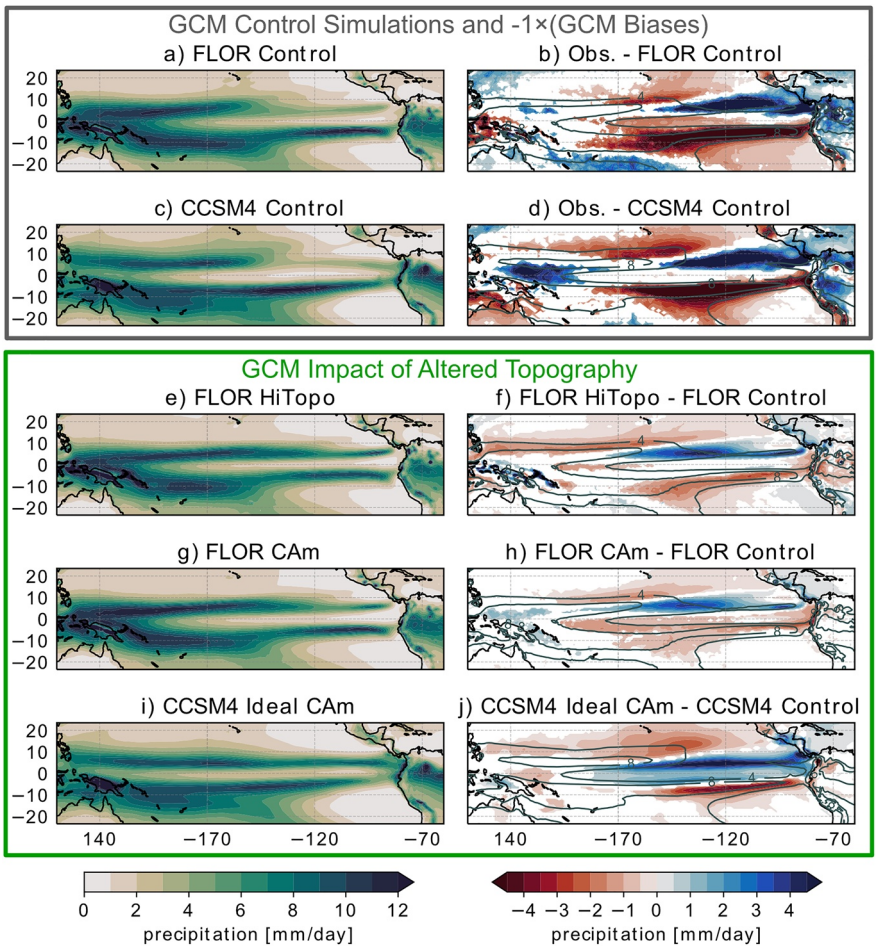

Figure 5. Influence of high orography on precipitation in the tropical Pacific for MAM. The left column shows MAM seasonal mean precipitation over the tropical Pacific for each of the model runs—FLOR Control (a), CCSM4 Control (c), FLOR HiTopo (e), FLOR CAm (g), and CCSM4 Ideal CAm (i). The right column shows differences between MAM seasonal mean precipitation for observations versus Control simulations–Obs. versus FLOR Control (b), Obs. versus CCSM4 Control (d)– and altered orography versus Control simulations–FLOR HiTopo versus FLOR Control (f), FLOR CAm versus FLOR Control (h), CCSM4 Ideal CAm versus CCSM4 Control (j). In these right column difference panels (b, d, f, h, and j), the corresponding FLOR or CCSM4 Control simulation MAM precipitation climatology is contoured in dark gray-green, with contour labels in mm/day. In the right panels, differences that are not significant at a 90% level based on a two-sided *t*-test are masked white. CCSM4, Community Climate System Model version 4; FLOR, Forecast-Oriented Low Ocean Resolution; MAM, March–April–May.

anomaly just south of the equator that weakens the prevailing northeasterly winds and increases SSTs in this region (Mitchell & Wallace, 1992; Wallace et al., 1989) (Figures 3e–3j, Figure S3e–j)—a positive feedback that contributes to the reduced SST and precipitation biases in the eastern Pacific (Figure 2, Figure S5). Altogether, the seasonal and annual-mean double ITCZ bias seen in FLOR Control and CCSM4 Control is substantially mitigated in FLOR HiTopo, FLOR CAm, and FLOR Ideal CAm, indicating that orographic height over Central America plays a key role in tropical eastern Pacific Ocean and atmosphere circulation, SSTs, and ITCZ position in the present climate. Additionally, comparing FLOR HiTopo and FLOR CAm, Central American orography appears to contribute more to the East Pacific climate biases than the orography in other regions such as the Andes, which are thought to play a major role in shaping the climate of this region (Takahashi & Battisti, 2007).

GCMs with improved climatologies, achieved for example through flux-adjustment or improved process representation, generally exhibit improved ENSO characteristics (Choi, 2015; Delworth et al., 2020; Krishnamurthy et al., 2015; Vecchi et al., 2014). In line with this prior result, we find that the raised orography

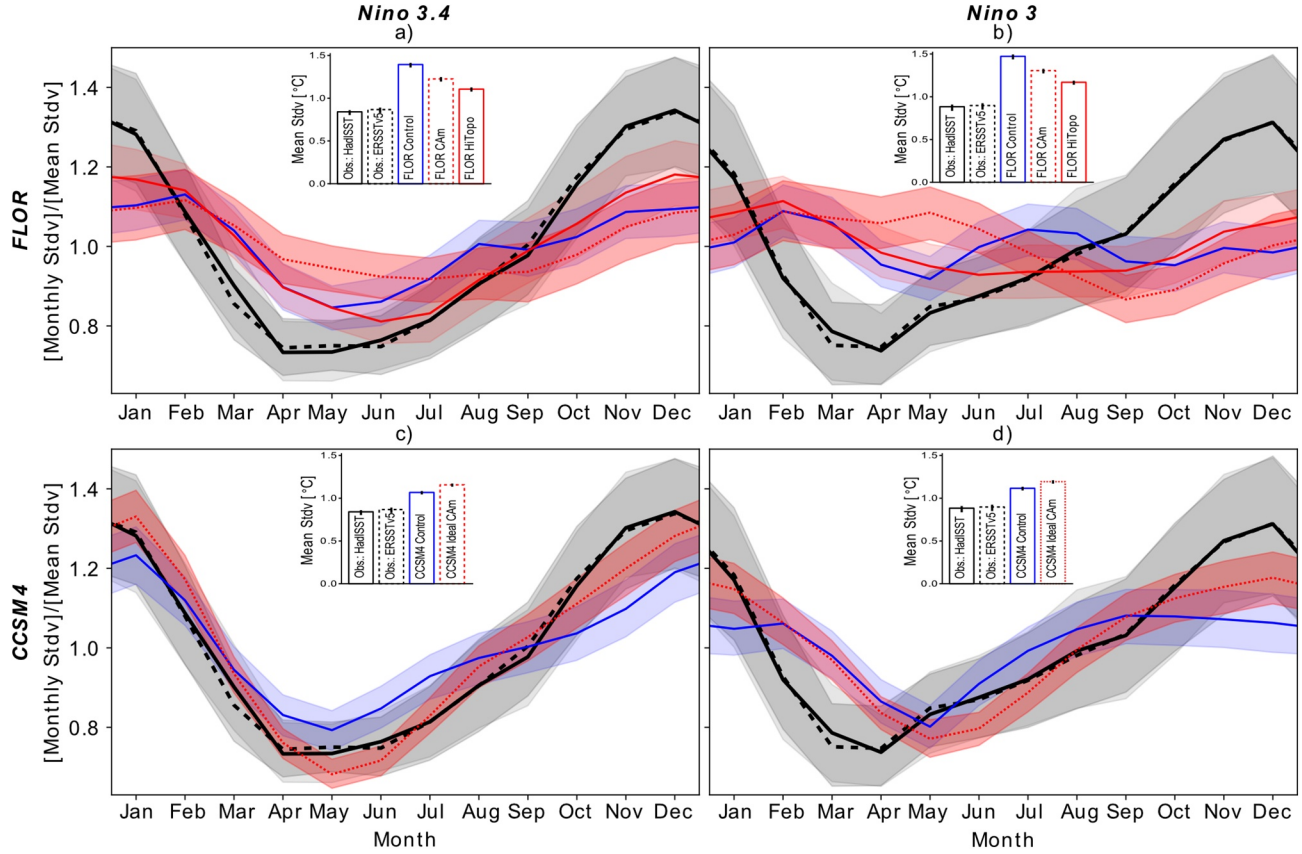

Figure 6. Seasonal cycle of ENSO variance. Standard deviation of ENSO SST anomalies as a function of month normalized by mean standard deviation (line plots) and the mean standard deviation of ENSO SST anomalies (bar plots within each panel) are plotted for the Niño 3.4 index (left column), and the Niño 3 index (right column). In all panels, HadISST observations are shown in solid black and ERSSTv5 observations are shown in dashed black. In the top row, FLOR results are shown (FLOR Control is blue, FLOR CAm is dashed red, and FLOR HiTopo is solid red), while in the bottom row CCSM4 results are shown (CCSM4 Control is blue, CCSM4 Ideal CAm is dashed red). For the seasonal cycle, error bars are translucent shading in the same color as the line plot, while for the mean variance error bars are black lines. In both cases, errors are bootstrapped 90% confidence intervals calculated from 1,000 re-samples of each data set. CCSM4, Community Climate System Model version 4; ENSO, El Niño-Southern Oscillation; FLOR, Forecast-Oriented Low Ocean Resolution; SST, sea surface temperature.

simulations improve several aspects of the models' ENSO variability. Most notably, in the raised orography simulations of both FLOR and CCSM4, the amplitude of ENSO's seasonal cycle of variance (normalized by total variance) increases to be more in line with observations (Figure 6). The phasing in the seasonality of ENSO is also somewhat improved when compared to observations (Figure 6). Additionally, the overall magnitude of ENSO variance is reduced to be more in line with observations in FLOR HiTopo and FLOR CAm compared to FLOR Control (interior barplots in Figures 6a and 6b; and Figure S6a,b). This improvement in magnitude is not seen in CCSM4 Ideal CAm compared to CCSM4 Control, though the magnitude of the variance bias is notably weaker in CCSM4 Control than in FLOR Control (Figures 6c and 6d and Figure S6c,d). In contrast to the seasonal cycle, phasing, and magnitude of variance, the low bias in Niño 3/3.4 SST anomaly skewness seen in both FLOR and CCSM4 Controls does not improve with elevated orography (not shown). The ENSO simulated by FLOR HiTopo is more similar to that observed than FLOR CAm, suggesting that the Central American orography, Andes, and perhaps even further remote orography, all play roles in shaping ENSO.

Outside the tropical Pacific, the raised FLOR HiTopo orography leads to improvements elsewhere, including over land. GCMs including FLOR often exhibit wet biases in precipitation over western North America (Johnson et al., 2020; van der Wiel et al., 2016). While these precipitation biases are partially attributable to SST biases (Johnson et al., 2020), we find that the artificially low GCM orography also substantially contributes to these precipitation biases. In FLOR HiTopo compared to FLOR Control, the wet bias in western

North America is significantly reduced, leading to a more accurate spatial distribution of precipitation (Figure S7). These biases are partially connected to SST improvements that are also seen in the FLOR CAm experiment, but mainly arise due to orographic changes outside of Central America. There are a few possible reasons for this change, including higher Rocky Mountains presenting a more significant barrier for the Great Plains Low Level Jet and Pacific storm track, shifts in atmospheric wave patterns or the westerly jet from elevated orography across the world, or more realistic ENSO teleconnections. We leave disentangling these dynamics to future work.

4. Discussion & Conclusions

Altogether, these experiments provide strong evidence that orography plays a key role in shaping the climate of the tropical East Pacific, and that overly smoothed orography in GCMs leads to substantial biases in this region. Central American orography blocks the flow of easterlies into the northeastern tropical Pacific, warming this region through reduced air-sea fluxes and ocean upwelling and an enhanced NECC, which in turn leads to enhanced precipitation. Insufficiently high orography in Central and South America leads the northeastern tropical Pacific to be biased cool and dry, with a weakened NECC, and the southeastern tropical Pacific to be biased wet (especially in the lower resolution CCSM4), substantially enhancing the double ITCZ bias. Prior work has demonstrated that the Andes interact with the zonal flow to create subsidence of dry air to their west, which increases latent heat fluxes and cools the southeastern tropical Pacific, reducing precipitation there (Takahashi & Battisti, 2007). Comparing FLOR HiTopo and FLOR CAm results, elevating Central American orography plays a more influential role in reducing the biases in eastern Pacific climatology than does elevating the Andes.

The low orography present in GCMs also leads to biases in ENSO simulation. Both in CCSM4 and in FLOR, increased orographic blocking causes greater seasonality in ENSO variance (Figure 6) that is more in line with that observed. This improvement is likely due to a northward shift in the climatological precipitation centroid in the eastern Pacific in MAM (i.e., reduction in the double ITCZ bias), which results in an enhanced annual harmonic in the climatology of the equatorial atmosphere-ocean system in the deep tropics (and a reduction in the semi-annual harmonic [Giese & Carton, 1994]). A variety of mechanisms closely link the climatological seasonal cycle of atmosphere-ocean coupling to ENSO, as the seasonal cycle of atmosphere-ocean coupling forces Rossby and Kelvin waves which amplify and terminate ENSO events (Battisti, 1988; Thompson & Battisti, 2000, 2001). Additionally, the termination of ENSO events has been tied to meridional shifts of westerly wind anomalies caused by seasonal movement of the warmest SSTs (Harrison & Vecchi, 1999; McGregor et al., 2013; Spencer, 2004; Vecchi & Harrison, 2003, 2006). Altogether, the low orographic peaks present in GCMs likely bias ENSO by enhancing tropical Pacific mean state biases.

When a GCM is developed, the model parameters are tuned to generate the most accurate possible simulation of climate given the model structure. Because FLOR and CCSM4 were optimized around their Control orography, the notable improvements in tropical climatology and variability are striking in the raised orography experiments, as they occur without any effort to re-tune the GCMs. We expect that even greater improvements could be possible if a GCM was developed and tuned with the raised orography.

These results suggest a logical pathway for reducing tropical biases in climate models, starting with a physically based change in how orography is prescribed in the models to better retain mountain peak heights. Our results show that this change in isolation can significantly affect major, long-standing biases in the simulated tropical climatology and interannual variability. The development of subgridscale parameterizations (such as clouds and subgridscale boundary layer processes in the atmosphere and ocean) would likely benefit if performed within models with a more realistic representation of the effective height of mountains. Additionally, experiments altering Central American orography in the lower resolution CCSM4 suggest that HiTopo-style orographic boundary conditions can improve GCMs with a range of spatial resolutions. Alternative interpolations to better retain orographic height may be beneficial for a variety of studies using high-end climate models, including global warming simulations, seasonal forecasting, and more idealized experiments, such as those examining the climatic role of orography. Indeed, variations in orographic boundary conditions over Central America have already been shown to substantially alter the response of the ITCZ to North Atlantic meltwater forcing (Atwood et al., 2020).

In examining the large scales of atmospheric and oceanic circulation where GCMs excel, HiTopo confers numerous advantages to both the tropical mean climatology, its variability, and its teleconnections. However, it is important to note that HiTopo orography should not be expected to lead to a more realistic climate simulation in all regards. In particular, HiTopo orography could lead to degradation in the representation of very local climate effects around orography, by creating overly broad regions at mountain peak elevation and some unrealistically steep mountain slopes. Further, HiTopo orography should not be expected to correct biases that have a different root cause, such as inaccurate clouds or ocean mixing.

This work suggests some useful directions for future work. First, future studies should seek practical ways to better capture the mechanical blocking of Central American orography in GCMs. In this study we explored one possible alternative interpolation scheme for topography (HiTopo) which replaces grid-cell averages with grid-cell maximums of surface height. Future studies might explore a range of interpolation methods to find an optimal interpolation of topography onto model grids to better capture the underestimated mechanical blocking effects of orography and minimize biases in simulated climate. A different but perhaps complementary method for resolving this issue could be improving subgridscale parameterizations of orographic drag and blocking, which is a topic of ongoing work at major modeling centers such as GFDL and NCAR (Elvidge et al., 2019). Continued increases in model resolution should also reduce these biases, but due to computational limitations may not occur at a rate commensurate with the importance of these biases for global climate. Second, given the improved tropical East Pacific climatology in our HiTopo simulations, it should be explored whether climate change projections, especially of the Pacific, are altered with adequate representation of this mountain range. We are analyzing simulations exploring this climate change question for a forthcoming publication. Third, future work should continue to explore the impact of mountains in atmosphere-ocean coupled models. While some other studies have used atmosphere-ocean coupled GCMs to explore the impact of mountains on climate (e.g., Abe et al., 2013; J. Baldwin & Vecchi, 2016; J. W. Baldwin et al., 2019; Kitoh, 1997, 2002), many studies which alter mountains in GCMs still just employ atmosphere-only experiments. In our study, most of the tropical Pacific improvements were discovered due to using GCMs with atmosphere-ocean coupling, highlighting the importance of considering atmosphere-ocean interactions in experiments altering mountains.

5. Conflict of Interest

The authors declare no conflicts of interest relevant to this study.

Acknowledgments
This work was supported in part by NOAA/OCO (award NA18OAR4310418), NOAA/MAPP (award NA18OAR4310273), and the Carbon Mitigation Initiative (CMI) at Princeton University. J. W. Baldwin was also funded by the Lamont-Doherty Earth Observatory Postdoctoral Fellowship. D. S. Battisti was funded by a gift from the Tamaki Foundation. Support was provided to A. R. Atwood by the National Science Foundation Paleo Perspective on Climate Change (P2C2) Grant AGS-1702827, and a fellowship from the National Oceanic and Atmospheric Administration Climate and Global Change Postdoctoral Program. We would like to acknowledge high-performance computing support from Cheyenne (https://doi.org/10.5065/D6RX99HX) provided by NCAR's Computational and Information Systems Laboratory, sponsored by the National Science Foundation. The authors are grateful to Kris Karnauskas and Isla Simpson for their insightful comments that greatly improved the manuscript.

Data Availability Statement

The output from the CCSM4 pre-industrial control run was obtained from the National Center for Atmospheric Research's (NCAR) High Performance Storage System (HPSS), which is available through the NCAR Data Sharing Service (https://www2.cisl.ucar.edu/resources/storage-and-file-systems/using-the-ncar-data-sharing-service). The location and details of this simulation can be found here: https://www.cesm.ucar.edu/experiments/cesm1.0/. The GFDL FLOR simulations were performed on computational resources managed and supported by Princeton Research Computing, a consortium of groups including the Princeton Institute for Computational Science and Engineering (PICSciE) and the Office of Information Technology's High Performance Computing Center and Visualization Laboratory at Princeton University. The source code for the GFDL CM2.5 (FLOR) is freely available at https://www.gfdl.noaa.gov/cm2-5-and-flor. Model and observational data used in this paper's analysis is permanently accessible at https://doi.org/10.5281/zenodo.4619128, and code to make the paper figures from this data is available at https://doi.org/10.5281/zenodo.4632489.

References

Abe, M., Hori, M., Yasunari, T., & Kitoh, A. (2013). Effects of the Tibetan Plateau on the onsetof the summer monsoon in South Asia: The role of the air-sea interaction. *Journal of Geophysical Research: Atmosphere*, *118*(4), 1760–1776. https://doi.org/10.1002/jgrd.50210

Adler, R. F., Huffman, G. J., Chang, A., Ferraro, R., Xie, P.-P., Janowiak, J., et al. (2003). The version-2 global precipitation climatology project (GPCP) monthly precipitation analysis (1979-present). *Journal of Hydrometeorology*, *4*(6), 1147–1167. https://doi.org/10.1175/1525-7541(2003)004%3C1147:TVGPCP%3E2.0.CO;2

Atwood, A. R., Donohoe, A., Battisti, D. S., Liu, X., & Pausata, F. S. R. (2020). Robust longitudinally variable responses of the ITCZ to a myriad of climate forcings. *Geophysical Research Letters*, *47*(17), e2020GL088833. https://doi.org/10.1029/2020GL088833

Baldwin, J., & Vecchi, G. (2016). Influence of the Tian Shan on Arid Extratropical Asia. *Journal of Climate*, *29*(16), 5741–5762. https://doi.org/10.1175/jcli-d-15-0490.1

Baldwin, J. W., Vecchi, G. A., & Bordoni, S. (2019). The direct and ocean-mediated influence of Asian orography on tropical precipitation and cyclones. *Climate Dynamics*, *53*(1-2), 805–824. https://doi.org/10.1007/s00382-019-04615-5

Battisti, D. S. (1988). Dynamics and thermodynamics of a warming event in a coupled tropical atmosphere–ocean model. *Journal of the Atmospheric Sciences*, *45*(20), 2889–2919. https://doi.org/10.1175/1520-0469(1988)045⟨2889:DATOAW⟩2.0.CO;2

Bonjean, F., & Lagerloef, G. S. (2002). Diagnostic model and analysis of the surface currents in the tropical Pacific Ocean. *Journal of Physical Oceanography*, *32*(10), 2938–2954. https://doi.org/10.1175/1520-0485(2002)032<2938:dmaaot>2.0.co;2

Boos, W. R., & Kuang, Z. (2010). Dominant control of the South Asian monsoon by orographic insulation versus plateau heating. *Nature*, *463*(7278), 218–222. https://doi.org/10.1038/nature08707

Chan, D., & Huybers, P. (2020). Identifying and correcting the World War 2 warm anomaly in sea surface temperature measurements. EarthArXiv. https://doi.org/10.31223/osf.io/ju26e

Chelton, D. B., Schlax, M. G., Freilich, M. H., & Milliff, R. F. (2004). Satellite measurements reveal persistent small-scale features in ocean winds. *Science*, *303*(5660), 978–983. https://doi.org/10.1126/science.1091901

Chiang, J. C. H., Fung, I. Y., Wu, C.-H., Cai, Y., Edman, J. P., Liu, Y., et al. (2015). Role of seasonal transitions and westerly jets in East Asian paleoclimate. *Quaternary Science Reviews*, *108*, 111–129. https://doi.org/10.1016/j.quascirev.2014.11.009

Choi, K. Y. (2015). El Niño-Southern Oscillation: Asymmetry, nonlinear atmospheric response and the role of mean climate (PhD Thesis). Princeton University.

Delworth, T. L., Cooke, W. F., Adcroft, A., Bushuk, M., Chen, J.-H., Dunne, K. A., et al. (2020). SPEAR: The Next Generation GFDL Modeling System for Seasonal to Multidecadal Prediction and Projection. *Journal of Advances in Modeling Earth Systems*, *12*(3), e2019MS001895. https://doi.org/10.1029/2019MS001895

Deser, C., Phillips, A. S., Tomas, R. A., Okumura, Y. M., Alexander, M. A., Capotondi, A., et al. (2012). ENSO and Pacific Decadal Variability in the Community Climate System Model Version 4. *Journal of Climate*, *25*(8), 2622–2651. https://doi.org/10.1175/JCLI-D-11-00301.1

Elvidge, A. D., Sandu, I., Wedi, N., Vosper, S. B., Zadra, A., Boussetta, S., et al. (2019). Uncertainty in the representation of orography in weather and climate models and implications for parameterized drag. *Journal of Advances in Modeling Earth Systems*, *11*(8), 2567–2585. https://doi.org/10.1029/2019MS001661

Fu, D., Chang, P., & Patricola, C. M. (2017). Intrabasin variability of East Pacific tropical cyclones during ENSO regulated by Central American gap winds. *Scientific Reports*, *7*(1), 1658. https://doi.org/10.1038/s41598-017-01962-3

Gelaro, R., McCarty, W., Suárez, M. J., Todling, R., Molod, A., Takacs, L., et al. (2017). The modern-era retrospective analysis for research and applications, version 2 (MERRA-2). *Journal of Climate*, *30*(14), 5419–5454. https://doi.org/10.1175/jcli-d-16-0758.1

Gent, P. R., Danabasoglu, G., Donner, L. J., Holland, M. M., Hunke, E. C., Jayne, S. R., et al. (2011). The Community Climate System Model Version 4. *Journal of Climate*, *24*(19), 4973–4991. https://doi.org/10.1175/2011JCLI4083.1

Giese, B. S., & Carton, J. A. (1994). The seasonal cycle in coupled ocean-atmosphere model. *Journal of Climate*, *7*(8), 1208–1217. https://doi.org/10.1175/1520-0442(1994)007<1208:tscico>2.0.co;2

Harrison, D. E., & Vecchi, G. A. (1999). On the termination of El Niño. *Geophysical Research Letters*, *26*(11), 1593–1596. https://doi.org/10.1029/1999GL900316

Holton, J. R. (1973). An introduction to dynamic meteorology. *American Journal of Physics*, *41*(5), 752–754. https://doi.org/10.1119/1.1987371

Hoskins, B. J., & Karoly, D. J. (1981). The steady linear response of a spherical atmosphere to thermal and orographic forcing. *Journal of the Atmospheric Sciences*, *38*(6), 1179–1196. https://doi.org/10.1175/1520-0469(1981)038<1179:tslroa>2.0.co;2

Huang, B., Thorne, P. W., Banzon, V. F., Boyer, T., Chepurin, G., Lawrimore, J. H., et al. (2017). Extended reconstructed sea surface temperature, version 5 (ERSSTv5): Upgrades, validations, and intercomparisons. *Journal of Climate*, *30*(20), 8179–8205. https://doi.org/10.1175/jcli-d-16-0836.1

Huffman, G., Bolvin, D., Braithwaite, D., Hsu, K., Joyce, R., & Xie, P. (2020). *Integrated multi-satellite retrievals for GPM (IMERG) version 4.4*. NASA's Precipitation Processing Center. https://doi.org/10.5194/egusphere-egu2020-5282

Hurrell, J. W., Holland, M. M., Gent, P. R., Ghan, S., Kay, J. E., Kushner, P. J., et al. (2013). The Community Earth System Model: A Framework for Collaborative Research. *Bulletin of the American Meteorological Society*, *94*(9), 1339–1360. https://doi.org/10.1175/BAMS-D-12-00121.1

Jarraud, M., Simmons, A., & Kanamitsu, M. (1986). *The concept, implementation and impact of an envelope orography* (ECMWF Vol. 2, pp. 81–128). Reading Publisher.

Jia, L., Vecchi, G. A., Yang, X., Gudgel, R. G., Delworth, T. L., Stern, W. F., et al. (2016). The roles of radiative forcing, sea surface temperatures, and atmospheric and land initial conditions in US summer warming episodes. *Journal of Climate*, *29*(11), 4121–4135. https://doi.org/10.1175/jcli-d-15-0471.1

Jia, L., Yang, X., Vecchi, G. A., Gudgel, R. G., Delworth, T. L., Rosati, A., et al. (2014). Improved seasonal prediction of temperature and precipitation over land in a high-resolution GFDL climate model. *Journal of Climate*, *28*(5), 2044–2062. https://doi.org/10.1175/JCLI-D-14-00112.1

Johnson, N. C., Krishnamurthy, L., Wittenberg, A. T., Xiang, B., Vecchi, G. A., Kapnick, S., & Pascale, S. (2020). The impact of sea surface temperature biases on North American precipitation in a high-resolution climate model. *Journal of Climate*. https://doi.org/10.1175/JCLI-D-19-0417.1

Karnauskas, K. B. (2014). Arctic forcing of decadal variability in the tropical Pacific Ocean in a high-resolution global coupled GCM. *Climate Dynamics*, *42*(11-12), 3375–3388. https://doi.org/10.1007/s00382-013-1836-3

Karnauskas, K. B., Busalacchi, A. J., & Murtugudde, R. (2008). Low-frequency variability and remote forcing of gap winds over the east Pacific warm pool. *Journal of Climate*, *21*(19), 4901–4918. https://doi.org/10.1175/2008jcli1771.1

Kessler, W. S. (2006). The circulation of the eastern tropical Pacific: A review. *Progress in Oceanography*, *69*(2), 181–217. https://doi.org/10.1016/j.pocean.2006.03.009

Kitoh, A. (1997). Mountain uplift and surface temperature changes. *Geophysical Research Letters*, *24*(2), 185–188. https://doi.org/10.1029/96gl03953

Kitoh, A. (2002). Effects of large-scale mountains on surface climate—A coupled ocean-atmosphere general circulation model study. *Journal of the Meteorological Society of Japan. Ser. II*, *80*(5), 1165–1181. https://doi.org/10.2151/jmsj.80.1165

Kong, W., & Chiang, J. C. (2020). Interaction of the westerlies with the Tibetan Plateau in determining the mei-yu termination. *Journal of Climate*, *33*(1), 339–363. https://doi.org/10.1175/jcli-d-19-0319.1

Krishnamurthy, L., Vecchi, G. A., Msadek, R., Wittenberg, A., Delworth, T. L., & Zeng, F. (2015). The seasonality of the Great Plains low-level jet and ENSO relationship. *Journal of Climate*, *28*(11), 4525–4544. https://doi.org/10.1175/JCLI-D-14-00590.1

Krishnamurthy, L., Vecchi, G. A., Yang, X., van der Wiel, K., Balaji, V., Kapnick, S. B., et al. (2018). Causes and probability of occurrence of extreme precipitation events like Chennai 2015. *Journal of Climate*. https://doi.org/10.1175/JCLI-D-17-0302.1

McGregor, S., Ramesh, N., Spence, P., England, M. H., McPhaden, M. J., & Santoso, A. (2013). Meridional movement of wind anomalies during ENSO events and their role in event termination. *Geophysical Research Letters*, *40*(4), 749–754. https://doi.org/10.1002/grl.50136

Mitchell, T. P., & Wallace, J. M. (1992). The annual cycle in equatorial convection and sea surface temperature. *Journal of Climate*, *5*(10), 1140–1156. https://doi.org/10.1175/1520-0442(1992)005⟨1140:TACIEC⟩2.0.CO;2

Molnar, P., Boos, W. R., & Battisti, D. S. (2010). Orographic controls on climate and paleoclimate of Asia: Thermal and mechanical roles for the Tibetan Plateau. *Annual Review of Earth and Planetary Sciences*, *38*(1), 77. https://doi.org/10.1146/annurev-earth-040809-152456

Oueslati, B., & Bellon, G. (2015). The double ITCZ bias in CMIP5 models: Interaction between SST, large-scale circulation and precipitation. *Climate Dynamics*, *44*(3-4), 585–607. https://doi.org/10.1007/s00382-015-2468-6

Putman, W. M., Lin, S.-J. (2007). Finite-volume transport on various cubed-sphere grids. *Journal of Computational Physics*, *227*(1), 55–78. https://doi.org/10.1016/j.jcp.2007.07.022

Rayner, N. A., Parker, D. E., Horton, E. B., Folland, C. K., Alexander, L. V., Rowell, D. P., et al. (2003). Global analyses of sea surface temperature, sea ice, and night marine air temperature since the late nineteenth century. *Journal of Geophysical Research: Atmosphere*, *108*(D14). https://doi.org/10.1029/2002jd002670

Reid, R. O. (1948). The equatorial currents of the eastern Pacific as maintained by the stress of the wind. *Journal of Marine Research*, *7*(2), 74–99.

Samanta, D., Karnauskas, K. B., & Goodkin, N. F. (2019). Tropical Pacific SST and ITCZ biases in climate models: Double trouble for future rainfall projections? *Geophysical Research Letters*, *46*(4), 2242–2252. https://doi.org/10.1029/2018GL081363

Shi, Z., Sha, Y., & Liu, X. (2016). Effect of Yunnan–Guizhou Topography at the Southeastern Tibetan Plateau on the Indian Monsoon. *Journal of Climate*, *30*(4), 1259–1272. https://doi.org/10.1175/JCLI-D-16-0105.1

Song, F., & Zhang, G. J. (2020). The impacts of horizontal resolution on the seasonally dependent biases of the Northeastern Pacific ITCZ in coupled climate models. *Journal of Climate*, *33*(3), 941–957. https://doi.org/10.1175/JCLI-D-19-0399.1

Spencer, H. (2004). Role of the atmosphere in seasonal phase locking of El Niño. *Geophysical Research Letters*, *31*(24). https://doi.org/10.1029/2004GL021619

Steenburgh, W. J., Schultz, D. M., & Colle, B. A. (1998). The structure and evolution of gap outflow over the Gulf of Tehuantepec, Mexico. *Monthly Weather Review*, *126*(10), 2673–2691. https://doi.org/10.1175/1520-0493(1998)126⟨2673:TSAEOG⟩2.0.CO;2

Sun, F., Yu, J.-Y. (2006). Impacts of Central America gap winds on the SST annual cycle in the eastern Pacific warm pool. *Geophysical Research Letters*, *33*(6). https://doi.org/10.1029/2005GL024700

Sverdrup, H. U. (1947). Wind-driven currents in a Baroclinic Ocean; with application to the equatorial currents of the Eastern Pacific. *Proceedings of the National Academy of Sciences of the United States of America*, *33*(11), 318–326. https://doi.org/10.1073/pnas.33.11.318

Takahashi, K., Battisti, D. S. (2007). Processes controlling the mean tropical Pacific precipitation pattern. Part II: The SPCZ and the southeast Pacific dry zone. *Journal of Climate*, *20*(23), 5696–5706. https://doi.org/10.1175/2007jcli1656.1

Thompson, C. J., & Battisti, D. S. (2000). A Linear Stochastic Dynamical Model of ENSO. Part I: Model Development. *Journal of Climate*, *13*(15), 2818–2832. https://doi.org/10.1175/1520-0442(2000)013⟨2818:ALSDMO⟩2.0.CO;2

Thompson, C. J., & Battisti, D. S. (2001). A linear stochastic dynamical model of ENSO. Part II: Analysis. *Journal of Climate*, *14*(4), 445–466. https://doi.org/10.1175/1520-0442(2001)014<0445:alsdmo>2.0.co;2

Valdes, P. J., & Hoskins, B. J. (1991). Nonlinear orographically forced planetary waves. *Journal of the Atmospheric Sciences*, *48*(18), 2089–2106. https://doi.org/10.1175/1520-0469(1991)048<2089:nofpw>2.0.co;2

van der Wiel, K., Kapnick, S. B., Vecchi, G. A., Cooke, W. F., Delworth, T. L., Jia, L., et al. (2016). The resolution dependence of contiguous U.S. precipitation extremes in response to CO2 forcing. *Journal of Climate*, *29*(22), 7991–8012. https://doi.org/10.1175/jcli-d-16-0307.1

Vecchi, G. A., Delworth, T., Gudgel, R., Kapnick, S., Rosati, A., Wittenberg, A. T., et al. (2014). On the seasonal forecasting of regional tropical cyclone activity. *Journal of Climate*, *27*(21), 7994–8016. https://doi.org/10.1175/jcli-d-14-00158.1

Vecchi, G. A., & Harrison, D. E. (2003). On the termination of the 2002–03 El Niño event. *Geophysical Research Letters*, *30*(18). https://doi.org/10.1029/2003GL017564

Vecchi, G. A., & Harrison, D. E. (2006). The Termination of the 1997–98 El Niño. Part I: Mechanisms of Oceanic Change. *Journal of Climate*, *19*(12), 2633–2646. https://doi.org/10.1175/JCLI3776.1

Wallace, J. M., Mitchell, T. P., & Deser, C. (1989). The influence of sea-surface temperature on surface wind in the Eastern Equatorial Pacific: Seasonal and interannual variability. *Journal of Climate*, *2*(12), 1492–1499. https://doi.org/10.1175/1520-0442(1989)002⟨3B1492:TIOSST⟩2.0.CO;2

Wallace, J. M., Tibaldi, S., & Simmons, A. J. (1983). Reduction of systematic forecast errors in the ECMWF model through the introduction of an envelope orography. *Quarterly Journal of the Royal Meteorological Society*, *109*(462), 683–717. https://doi.org/10.1002/qj.49710946202

White, R. H., Battisti, D. S., & Roe, G. H. (2017). Mongolian Mountains Matter Most: Impacts of the latitude and height of Asian orography on Pacific wintertime atmospheric circulation. *Journal of Climate*, *30*. https://doi.org/10.1175/jcli-d-16-0401.1

Xie, P., & Arkin, P. A. (1997). Global precipitation: A 17-year monthly analysis based on gauge observations, satellite estimates, and numerical model outputs. *Bulletin of the American Meteorological Society*, *78*(11), 2539–2558. https://doi.org/10.1175/1520-0477(1997)078<2539:gpayma>2.0.co;2

Xie, S.-P., Miyama, T., Wang, Y., Xu, H., Szoeke, S. P. d., Small, R. J. O., et al. (2007). A regional ocean–atmosphere model for Eastern Pacific climate: Toward reducing tropical biases. *Journal of Climate*, *20*(8), 1504–1522. https://doi.org/10.1175/JCLI4080.1

Xie, S.-P., Okumura, Y., Miyama, T., & Timmermann, A. (2008). Influences of Atlantic climate change on the tropical Pacific via the Central American Isthmus. *Journal of Climate*, *21*(15), 3914–3928. https://doi.org/10.1175/2008JCLI2231.1

Xie, S.-P., Xu, H., Kessler, W. S., & Nonaka, M. (2005). Air–sea interaction over the eastern Pacific warm pool: Gap winds, thermocline dome, and atmospheric convection. *Journal of Climate*, *18*(1), 5–20. https://doi.org/10.1175/jcli-3249.1

Xu, H., Xie, S.-P., Wang, Y., & Small, R. J. (2005). Effects of Central American Mountains on the Eastern Pacific Winter ITCZ and Moisture Transport. *Journal of Climate*, *18*(18), 3856–3873. https://doi.org/10.1175/JCLI3497.1

Xu, W. (2019). How South American topography influences climate simulation over the South Pacific Ocean in CESM. In *AGU Fall Meeting 2019*. AGU.